

One-axis twisting with nearest neighbour interactions

Edward Gheorghita

Supervised by: Dr. Ayaka Usui, Dr. Bruno Julia Diaz

A thesis presented for the degree of
Master of Science



Department of Physics
University of Barcelona
Barcelona, Spain
July 11th, 2022

Abstract

It is known that a maximally entangled state, GHZ state, is generated by the one-axis twisting Hamiltonian. Recently, it has been numerically shown that a Hamiltonian having neighboring interactions and a field only produces the same dynamics. It is intriguing because it was believed that all-with-all interactions are required for one-axis twisting. The purpose of this work is to reveal how such simple Hamiltonians can show the one-axis twisting and mimic all-with-all interactions. In particular, we apply the many-body protected manifold technique to the Heisenberg XXX model with a staggered field in attempt to recover all-with-all interactions. We begin with a thorough review of one-axis twisting without and with decoherence. Then, we introduce the many-body protected manifold technique and apply it to the Heisenberg XXZ model, which acquires all-with-all interactions and can generate one-axis twisting. We apply this technique to the Heisenberg XXX model.

Acknowledgements

I would like to first thank Dr. Ayaka Usui for agreeing to supervise my master's thesis. My previous research experience was in theoretical quantum optics, so I was nervous choosing a topic in cold-atom theory. My transition was bumpy, but her dedication and patience while guiding me through complicated topics truly enhanced my ability to both understand and appreciate the material – and I have her to thank for introducing me to this wonderful research area.

Next, I would like to thank Dr. Bruno Julia Diaz and the cold-atoms group at the University of Barcelona. The weekly meetings provided a great learning opportunity not only through sharing my work but by hearing others' research as well. This always resulted in interesting discussions and these are moments I will carry with me into the future.

Finally, I am indebted to my parents for their gracious love and support throughout my academic adventures. Without them, I would not be able to pursue my dreams and I cannot thank them enough for always believing in me.

Contents

1	Introduction	1
2	One-axis twisting	2
2.1	Mathematical formalism	2
2.2	OAT Hamiltonian and time evolution	4
2.3	Expectation value of collective spin operator	4
3	Decoherence	5
3.1	Single-particle dephasing	5
3.2	Expectation value for collective spin operators with decoherence	6
3.3	Fidelity of the system	7
4	Many-body protected manifold	8
4.1	Mathematical formalism	8
4.2	Analytical solution - perturbation theory	9
5	Heisenberg XXZ model	10
5.1	Collective spin operators	11
5.2	Projection into ground state manifold	11
6	Results	13
6.1	Recovering all-with-all interactions from Heisenberg XXZ	13
6.2	Heisenberg XXX model with staggered field	13
7	Conclusion	14
	Bibliography	16
A	Coherent spin states	18
B	Expectation value of collective spin operator	20
C	Fidelity calculation	21

1 Introduction

An effective method for studying many-body quantum physics is to trap cold atoms in an optical lattice. Experimentally, this provides flexibility that allows one to finely tune parameters such as periodic potential depth or interaction strength between particles - essentially researchers can tailor the system to their needs. Furthermore, trapped cold atoms can be represented by canonical Hamiltonians (such as the Bose-Hubbard model) allowing for relatively straightforward cross-checking between theory and experiment. The process of trapping the cold atoms begins by creating a lattice-like interference pattern with two laser beams i.e. a periodic potential. Then introducing the atoms imposes an AC-Stark interaction between the atoms and the electric field which makes the energy levels of the atoms dependent on the light intensity. In this way, one can trap the atoms in the optical lattice Ref.[BZ06, Rey21]. There are many practical applications of cold-atom lattices, however, for the purpose of this thesis, we focus on sensing and metrological uses. These are two platforms which not only utilize cold atoms trapped in optical lattices but they are also primary candidates for using one-axis twisting induced entanglement to enhance sensitivity Ref.[SHH21]. We briefly introduce inertial sensors and atomic clocks as two particular examples.

An atomic interferometer is known as the matter-wave counterpart to the optical Mach-Zehnder interferometer. Both optical and atomic interferometers are structured such that the incoming wave is split into two paths – one of which receives an additional phase shift. After a period of time or length, the two waves are then recombined producing an interference effect which can be measured typically via the difference in populations of states. More precisely, atomic interferometers obtain a phase shift when the interferometer accelerates making them ideal candidates for highly sensitive accelerometers, gravimeters, and gyroscopes Ref.[WPW99].

Atomic clocks currently provide the most precise measurement of any physical quantity, this of course being time. In particular, Caesium fountain clocks hold the standard in international time-keeping by maintaining a stability of one part in 10^{16} Ref.[LBY⁺15]. These devices function by comparing the ultra-stable frequency of an atomic transition in the microwave domain with the frequency of a local oscillator. Soon after microwave atomic clocks were introduced, it was postulated that clocks in the optical domain could produce an improvement of a factor of 10^6 . At that time, however, it was extremely difficult to measure the much fast oscillating frequencies in the optical domain Ref.[RGK⁺14]. This eventually was solved with the invention of a frequency comb which opened a wide variety of new atomic clock research including trapping ions in optical lattices.

The sensitivity of both systems mentioned above are fundamentally limited by the shot noise limit (SNL), that is, how precise one can measure a quantum mechanical observable. For interferometers, the observable is commonly mapped to a phase shift so the limit is defined as $\Delta\phi = \xi/\sqrt{N}$ where ξ is the squeezing parameter and N represents the number of particles. Classically, the lowest this limit can be is $1/\sqrt{N}$. However, by introducing squeezed states ($\xi < 1$) one can detect below this limit. For instance, recently the use of entangled states in atomic clocks achieved a metrological enhancement of 4.4 dB Ref.[PPCS⁺20]. On the other hand, squeezing has yet to demonstrate improvement for cold-atom inertial sensors.

Clearly, entanglement can be quite a valuable tool for the future development of cold-atom devices. The general purpose of this thesis is to study the generation and maintenance of entangled states in many-body spin-1/2 systems. In particular, we analyse why all-for-all interactions are produced by evolving nearest neighbour interacting Hamiltonians. The

remainder of this work is structured as follows. In Section 2, we provide an in-depth review of one-axis twisting. This is the fundamental technique used to generate squeezed states which we use throughout the paper. From Section 3-5, we closely follow the methods outlined in *Many-body protected entanglement generation in interacting spin systems* Ref.[RJF⁺08] which provide a framework for developing noise-resistant entangled states which can be used for optical lattice systems such as the Heisenberg XXZ model. Finally, in Section 5 we apply these techniques to the Heisenberg XXX model with a staggered field in an attempt to explain why squeezing occurs as was demonstrated numerically in Ref.[GUB21].

2 One-axis twisting

Measurements of quantum observables are inherently limited by the noise of the correlated quantum fluctuations in a system. For instance, in an optical system the phase and amplitude quadratures of the radiation field are conjugate variables in which the preciseness of their measurement is governed by the Heisenberg uncertainty principle (HUP). From the HUP, one finds the highest precision possible is obtained when the two conjugate variables are equal, also known as the standard quantum limit (SQL). To avoid this, one can introduce a squeezed radiation field making it possible to measure a conjugate variable below the SQL Ref.[XWK87]. Four-wave mixing is a common technique for generating a squeezed light source where one injects a weak probe beam and a pump into a ⁸⁵Rb vapor cell causing nonlinear interactions and thus the output beams become correlated Ref.[MBPL08]. Experiments have demonstrated the effectiveness of light-squeezing for various applications including but not limited to atomic force microscopy, gravitational wave detection, and spin-noise spectroscopy Ref.[LP18, AAA⁺13, LLMP19].

One can demonstrate similar noise-reduction techniques in collective spin systems through non-classical state preparations. In particular, we focus on pseudo spin-1/2 particles represented by two-level systems or qubits. Initially, we have a system of uncorrelated particles aligned in one direction where the uncertainty of the spin along an axis orthogonal to the mean spin vector equals the sum of each individual elementary spins. In this case, the SQL is defined as $J/2$ where J represents the total spin. However, introducing a nonlinear Hamiltonian produces an infinite range interaction between the particles creating correlations. The subsequent states are known as spin squeezed states (SSS) where the variance of one spin component normal to the mean spin vector can be less than the SQL. The SSS were first proposed by Kitagawa and Ueda in 1991, in which they showed the derivation and effects of one-axis twisting (OAT) and two-axis countertwisting Ref.[KU93]. Since then these have been studied extensively both in theory and experiments including but not limited to entanglement detection, spin squeezing in a Bose-Einstein condensate, and enhancement of optical atomic clocks Ref.[MWSN11].

2.1 Mathematical formalism

In this section, we introduce the necessary background for building a coherent spin state because allows us to easily demonstrate the spin-squeezing. Furthermore, these states are built in the coupled basis and it is important to understand the clear differences between this and the uncoupled basis which we introduce later. For the sake of brevity, we reserve the Appendix for the more rigorous derivations.

Collective spin operators:

In an ensemble of N identical spin-1/2 particles, there are 2^N orthogonal states. The directional components of collective spin operators and the total spin operator are defined respectively

$$\hat{J}_\alpha = \frac{1}{2} \sum_{i=0}^{N-1} \hat{\sigma}_i^\alpha, \quad (1)$$

$$\hat{J}^2 = \hat{J}_x^2 + \hat{J}_y^2 + \hat{J}_z^2, \quad (2)$$

where we use natural units ($\hbar = 1$), $\alpha = \{x, y, z\}$, and the i index denotes the position of the particle. The $\hat{\sigma}_i^\alpha$ operator represents the canonical Pauli matrices which obey the commutation relation $[\hat{\sigma}_j, \hat{\sigma}_k] = 2i\epsilon_{jkl}\hat{\sigma}_l$ where ϵ_{jkl} is the Levi-Civita symbol. The next operator we define is the creation spin operator because it is used in the following derivation for the Dicke state

$$\hat{J}_+ = \frac{1}{2} \sum_{i=0}^{N-1} \hat{\sigma}_i^+. \quad (3)$$

The creation operator Eq.(3) is also defined as $\hat{J}_+ = \hat{J}_x + i\hat{J}_y$.

Dicke state:

In order to build the coherent spin state, we need a well-defined state which acts as an eigenstate simultaneously to the operators \hat{J}_z and \hat{J}^2 . These states are known as Dicke states and can be constructed by applying the raising operator $(J + M)$ times on the ground state $|J, -J\rangle$ Ref.[Dic54]. They are defined as

$$|J, M\rangle = \frac{1}{(J - M)!} \binom{2J}{J + M}^{-1/2} (\hat{J}_+)^{(J+M)} |J, -J\rangle, \quad (4)$$

where $J = N/2, N/2 - 1, \dots, 0$ is the eigenvalue of total spin, and $M = -J, -J + 1, \dots, J - 1, J$ is the eigenvalue of \hat{J}_z . Notice this state is defined analogously to a Fock state in the conventional quantum mechanics formalism. With the angular momentum eigenstate defined, we provide the eigenvalue equations for the collective spin operators mentioned above

$$\hat{J}_z |J, M\rangle = M |J, M\rangle \quad (5)$$

$$\hat{J}^2 |J, M\rangle = J(J + 1) |J, M\rangle. \quad (6)$$

Coherent spin state:

In quantum optics, coherent states are desirable because they hold several important properties. First, they are minimum uncertainty states at the classical level - in the case of radiation fields $\Delta x \Delta p = \hbar/2$. Even more, coherent states are non-orthogonal, form an overcomplete basis, and fulfil the closure relation. With these properties, coherent states serve as an exceptional quantum representation of classical fields such as laser light. In 1972, Arrechi *et al.* Ref.[ACGT72] illustrated the relation between free atoms and radiation fields. They showed that it is possible to replicate every property mentioned above but with a system of free atoms - hence, the atomic coherent state. This state is derived by applying a rotation operator $\mathcal{R}_{\theta, \phi}$ to the ground state $|J, -J\rangle$ [Appendix A]

$$|\theta, \phi\rangle = \sum_{M=-J}^J \binom{2J}{J + M}^{1/2} \left(\cos \frac{\theta}{2}\right)^{(J+M)} \left(\sin \frac{\theta}{2}\right)^{(J-M)} e^{i(J+M)\phi} |J, M\rangle, \quad (7)$$

where θ and ϕ are the polar and azimuthal angles about the Bloch sphere, respectively. We recognize two important properties of the atomic coherent state which resemble the canonical coherent states mentioned above. First, the non-orthogonality of the states which in turn form an overcomplete basis

$$|\langle \theta, \phi | \theta', \phi' \rangle|^2 = \left[\cos \left(\frac{1}{2} \Theta \right) \right]^{4J}, \quad (8)$$

where $\cos \Theta = \cos \theta \cos \theta' + \sin \theta \sin \theta' \cos(\phi - \phi')$. Next, the minimum uncertainty property also holds for atomic coherent states

$$\langle \hat{J}_\xi^2 \rangle \langle \hat{J}_\nu^2 \rangle = \frac{1}{4} \langle \hat{J}_\delta \rangle^2, \quad (9)$$

where the spin operators have been rotated by $(\hat{J}_\xi, \hat{J}_\nu, \hat{J}_\delta) = \mathcal{R}_{\theta, \phi}(\hat{J}_x, \hat{J}_y, \hat{J}_z) \mathcal{R}_{\theta, \phi}^{-1}$. With the coherent spin state properly defined, we now fully utilize its properties to achieve spin squeezing.

2.2 OAT Hamiltonian and time evolution

One of the primary models for spin squeezing is the one-axis twisting Hamiltonian. This Hamiltonian introduces nonlinear infinite-range interactions to a spin system. The nonlinearity is essential because otherwise, linear interactions would simply only rotate the spins without producing any correlation between them. The OAT Hamiltonian is defined as

$$\hat{H}_z = \chi \hat{J}_z^2. \quad (10)$$

The simplicity of this Hamiltonian makes the time evolution of the system straightforward. We begin with aligning the initial state in the x -direction by setting the coherent spin state angles to $\theta = \pi/2$ and $\phi = 0$

$$|\pi/2, 0\rangle = 2^{-J} \sum_{M=-J}^J \binom{2J}{J+M}^{1/2} |J, M\rangle. \quad (11)$$

Now we apply the squeezing Hamiltonian to the initial state using the time-evolution operator $\hat{U}(t) = e^{-i\chi \hat{J}_z^2 t}$ which results in

$$|\psi(t)\rangle = 2^{-J} \sum_{M=-J}^J \binom{2J}{J+M}^{1/2} e^{-i\chi M^2 t} |J, M\rangle. \quad (12)$$

The Husimi-Q probability distribution is given by the function $Q(\theta, \phi) = |\langle \theta, \phi | \psi(t) \rangle|^2$ as seen in Figure 1.

2.3 Expectation value of collective spin operator

The effects of spin squeezing can also be demonstrated by calculating the expectation value of the collective spin operator with the SSS. In the next section, we use this result (an ideal system) as a comparison to a system with added noise. First, we calculate the time evolution of the spin operators because we are working in the Heisenberg picture [Appendix B]

$$\hat{J}_+(t) = \hat{J}_+(0) e^{i2\chi t (\hat{J}_z + 1/2)}. \quad (13)$$

We now have the squeezed operator and so the next step is to apply this to the coherent spin state aligned in the x -direction: $\langle \pi/2, 0 | \hat{J}_+(t) | \pi/2, 0 \rangle$ [Appendix B]. With the result

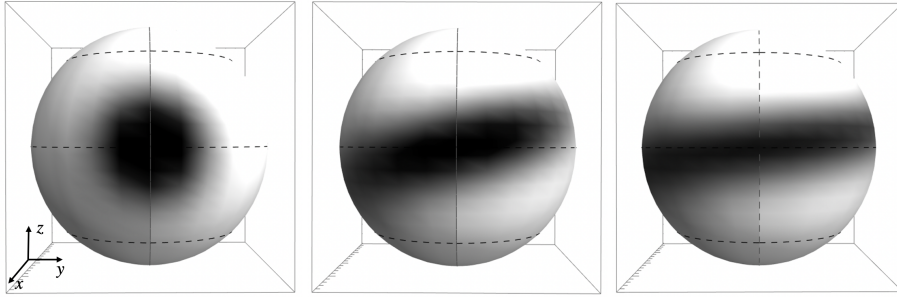


Figure 1: We map $Q(\theta, \phi)$ onto spherical coordinates using a Wolfram Mathematica package created by Juan José García Ripoll Ref.[Rip16]. In other words, the time evolution of the quasi-probability distribution for the spin squeezed state. From left to right the values for χt are 0, 0.199, 0.399.

of $\langle \hat{J}_+ \rangle$, we make the realization that $\langle J_x \rangle = \text{Re}[\langle J_+ \rangle]$ and so we have the final result for the expectation value of the x -spin operator in a squeezed spin state

$$\langle \hat{J}_x \rangle = J \cos^{2J-1} \frac{\mu}{2}. \quad (14)$$

Where $\mu = 2\chi t$. An important consequence is that at times $t = n\pi/2$, the expectation value will be zero, which supports the theory of maximally entangled states being generated from this Hamiltonian.

3 Decoherence

Decoherence is the process which transforms a quantum state into an apparent classical state through interactions with an external environment. In complete isolation, the "quantum nature" or coherence of the system remains unaffected. However, the true fragility of the system becomes apparent once it couples with an environment as it tends to rapidly lose its quantum behaviour. There are many studies of decoherence since it was initially outlined in 1991 Ref.[Zur02]. Notable experiments that study the effect of quantum decoherence include microwave cavity experiments Ref.[RBH01], decoherence of ions due to radiation Ref.[TKL+00], and matter-wave interferometers Ref.[HGH+12].

In this section, we follow the methods in Ref.[RJF+08] by first defining the type of decoherence attributed to this system. Then we provide a qualitative description of how the decoherence causes a depletion of the ground-state manifold. We then calculate the expectation value of \hat{J}_x with decoherence. This allows us to compare with our results from the above section with no decoherence. Finally, we determine the fidelity of the GHZ state generation with decoherence.

3.1 Single-particle dephasing

We define single-particle dephasing as the dominant source of noise which can result from internal collisions, stray fields and laser in-stabilities Ref.[HMP+97]. This process causes the off-diagonal density matrix elements to decay exponentially while maintaining the populations. To model the decoherence we follow the procedure in Ref.[RJF+08],

$$\hat{H}_{\text{env}} = \frac{1}{2} \sum_i h_i(t) \hat{\sigma}_i^z \quad (15)$$

where $h_i(t)$ are assumed to be independent stochastic Gaussian processes with zero mean. Furthermore, one can view the effect of dephasing in terms of the energy levels of the

Hamiltonians. For instance, because \hat{H}_{env} commutes with both \hat{J}_z and \hat{J}^2 , coupling between degenerate energy levels of \hat{H}_z is now possible. Thus, as the state evolves, transitions between different J subspaces are allowed causing a depletion of the initially populated ground-state manifold. See Figure 2. Consequently, the stability of the entangled states diminish as they require the symmetric properties of the ground-state manifold.

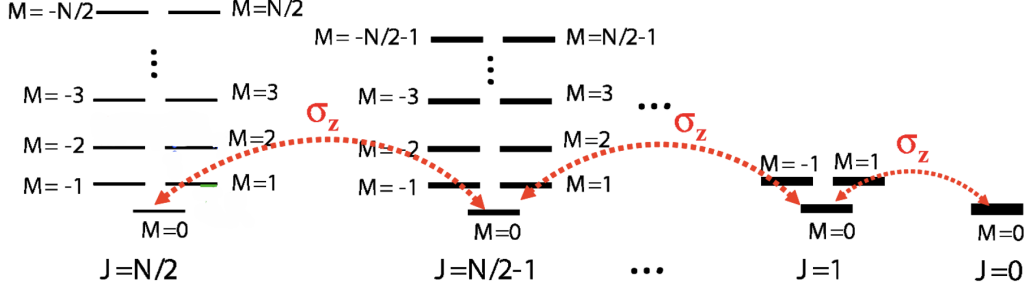


Figure 2: Illustration of the effect of single-particle dephasing where the Pauli operator couples states with different total spin J but same M . In a non-protected system, this leads to a depletion of the ground-state manifold $J = N/2$ Ref.[RJP⁺08].

3.2 Expectation value for collective spin operators with decoherence

One method for evaluating the effect of decoherence on the system is to calculate the expectation value of the collective spin operator. We then compare this calculation with the result Eq.(14) which was the expectation value of the same collective spin operator without the decoherence

$$\langle \hat{J}_x \rangle = \text{Tr} \left[\overline{\hat{J}_+ (0) \rho(t)} \right], \quad (16)$$

where the overbar denotes averaging over the different random outcomes which is necessary and is introduced because of the stochastic Gaussian term $h_i(t)$. Thus, we restrict the overbar to just the exponential term which contains $h_i(t)$. Note that the coupled spin basis $\{|J, M\rangle\}$ is not proper anymore since it does not diagonalize \hat{H}_{tot} . This is because \hat{H}_z commutes with both \hat{J}_z and \hat{J}^2 , but \hat{H}_{env} only commutes with \hat{J}_z . We switch to the more general uncoupled spin basis defined as $\{|n^{(k)}\rangle = |s_1^k, s_2^k, \dots, s_N^k\rangle\}$ where $s_i^k = \pm 1$ for \uparrow, \downarrow , and $k = 1, 2, \dots, 2^N$, and

$$\hat{\sigma}_i^z |s_1^k, s_2^k, \dots, s_N^k\rangle = s_i^k |s_1^k, s_2^k, \dots, s_N^k\rangle, \quad (17)$$

and the density matrix for this state is simply

$$\hat{\rho} = \sum_{k,l} \rho_{k,l}(0) |n^{(k)}\rangle \langle n^{(l)}|. \quad (18)$$

We define the time evolution operator in the uncoupled basis as

$$\hat{U}(t) = e^{-i \left[\chi (\sum_i \hat{\sigma}_i^z)^2 t + \frac{1}{2} \sum_{i=0}^{N-1} \int_0^t d\tau h_i(\tau) \hat{\sigma}_i^z \right]}. \quad (19)$$

Now, we use Eq.(19) to find Eq.(16) which results in

$$\langle \hat{J}_x \rangle = \sum_{k,l} \langle n^{(l)} | \rho_{k,l}(0) e^{-i\chi t/4 [(\sum_i s_i^k)^2 - (\sum_i s_i^l)^2]} e^{-i/2 \left[\sum_i \int_0^t d\tau h_i(\tau) (s_i^k - s_i^l) \right]} \hat{J}_+ |n^{(k)}\rangle. \quad (20)$$

To simplify this, we must recognize a crucial aspect of the raising operator – that is, in the uncoupled basis it only connects states with one spin flipped Eq.(3). In other words, the operator will flip one particle at a time of the k -state, so when this state connects with the l -state, $\sum_i (s_i^k - s_i^l)$ must equal -2 . The decoherent term becomes

$$e^{-i/2 \left[\sum_i \int_0^t d\tau h_i(\tau) (s_i^k - s_i^l) \right]} = \overline{e^{i \int_0^t d\tau h(\tau)}} = e^{-\Gamma(t)}, \quad (21)$$

where the property for Gaussian variables $\overline{\exp[-i \int_0^t d\tau h(\tau)]} = \exp[-\Gamma(t)]$ is provided in Ref.[RJF+08]. Therefore, the expression for the expectation value simplifies to

$$\langle \hat{J}_x \rangle = e^{-\Gamma(t)} \sum_{k,l} \langle n^{(l)} | \rho_{k,l}(0) e^{-i\chi t/4 [(\sum_i s_i^k)^2 - (\sum_i s_i^l)^2]} \hat{J}_+ | n^{(k)} \rangle.$$

We have effectively separated the decoherence term from the density matrix equation. This shows everything within the density matrix is now the expectation value for the spin operator with no decoherence, exactly representing the ideal case which we previously calculated. We represent this in a simpler fashion

$$\langle \hat{J}_x \rangle = e^{-\Gamma(t)} \langle \hat{J}_x \rangle_{\Gamma=0}. \quad (22)$$

The negative exponential acts as a decay to the expectation value of the operator with no decoherence. This shows us the detrimental effect the noise has on the system.

3.3 Fidelity of the system

The fidelity of two quantum states is a measure of the distance between them i.e. how closely related they are. We choose to compare an entangled state in an ideal system with an entangled state in a system with added decoherence. This shows us exactly how the decoherence effects the stability of the entangled state generation. In the following equation, the outer product states are the ideal cases (no decoherence). Note, t_0 is designated for the time when the entangled GHZ states are produced

$$\mathcal{F}(t_0) = \overline{\langle \psi_x^{\text{GHZ}} | \hat{\rho}(t_0) | \psi_x^{\text{GHZ}} \rangle} \quad (23)$$

where

$$\overline{\hat{\rho}(t_0)} = \sum_{k,l} \rho_{k,l}(0) e^{-i\chi t_0/4 [(\sum_i s_i^k)^2 - (\sum_i s_i^l)^2]} e^{-\frac{1}{2}\Gamma(t) \sum_i (s_i^k - s_i^l)} | n^{(k)} \rangle \langle n^{(l)} |. \quad (24)$$

Next, we solve for the GHZ state in the uncoupled basis with no decoherence $|\psi_x^{\text{GHZ}}\rangle$ which is straightforward because we already know the eigenvalue for $\hat{\sigma}_z$ when it is applied to an arbitrary state in the uncoupled basis. Thus,

$$|\psi_x^{\text{GHZ}}\rangle = \sum_k c_k(0) e^{-i\chi t_0/4 (\sum_i s_i^k)^2} | n^{(k)} \rangle. \quad (25)$$

Upon applying Eq.(25) to Eq.(24) we find several of the eigenvalue terms cancel and we then use statistical analysis to simplify the rest [Appendix C]. Finally we assert that at $t = 0$, the atoms are all polarized in the x direction, so $\rho_{k,l}(0) = 2^{-N}$. This results in the final equation for fidelity Ref.[RJF+08]

$$\mathcal{F}(t_0) = \left(\frac{1 + e^{-\Gamma(t_0)}}{2} \right)^N. \quad (26)$$

This informs us that this entanglement is more fragile for more particles. This also provides a viable comparison with systems we will discuss in the next chapter which attempt to increase the stability of the entanglement.

4 Many-body protected manifold

The many-body protected manifold (MPM) is a solution proposed by Ref.[R,JF+08] to reduce the effects of decoherence. The MPM is created by introducing an additional Hamiltonian in the coupled spin basis, which is defined as

$$\hat{H}_{\text{prot}} = -\lambda \hat{J}^{(0)2}. \quad (27)$$

The purpose for this protection is to isolate the ground-state manifold from the rest of the Hilbert space by including a finite energy gap $E_g = \lambda N$ which acts as a barrier between the degenerate states mentioned above. An important characteristic of this Hamiltonian that should be noted is when the system is in the MPM, \hat{H}_{prot} does not affect the dynamics of the squeezing because of the commutation relation $[\hat{H}_z, \hat{H}_{\text{prot}}] = 0$.

In this section, we first introduce the necessary mathematical formalism to utilize the MPM. Then we solve for the density matrix projected onto the MPM using perturbation theory. The result provides an analytical description of how the protection term reduces the decoherence.

4.1 Mathematical formalism

Prior to this section, we constrained the discussion to coupled spin states within the symmetric spin space $|J, M\rangle$. However, in order to completely label the set of 2^N possible states of the Hilbert space, we now introduce the quantum number β which distinguishes states that have equal J and M but different internal permutations. We denote the new basis as $|J, M, \beta\rangle$. For instance, for $N = 4$ we can write the coupled basis $|J = 1, M = 1, \beta = 1\rangle$ and $|J = 1, M = 1, \beta = 2\rangle$ as

$$\begin{aligned} |1, 1, 1\rangle &= \frac{1}{\sqrt{2}} (|\uparrow\uparrow\downarrow\downarrow\rangle - |\downarrow\downarrow\uparrow\uparrow\rangle) \\ |1, 1, 2\rangle &= \frac{1}{\sqrt{2}} (|\uparrow\downarrow\uparrow\downarrow\rangle - |\downarrow\uparrow\downarrow\uparrow\rangle). \end{aligned}$$

We introduce a new definition of collective spin operators, which Fourier transform Pauli operators on single particles,

$$\hat{J}_z^{(k)} = \frac{1}{2} \sum_j \hat{\sigma}_j^z e^{i2\pi jk/N}. \quad (28)$$

For example, when $N = 4$ we have $\hat{J}_z^{(0)} |2, 1\rangle = |2, 1\rangle$ but if we choose a different value for k ,

$$\hat{J}_z^{(2)} |2, 1\rangle = \frac{1}{\sqrt{2}} |1, 1, 1\rangle - \frac{1}{\sqrt{6}} |1, 1, 2\rangle + \frac{1}{\sqrt{3}} |1, 1, 3\rangle.$$

Finally, we re-write the definitions for all of the Hamiltonians in terms of the Fourier transform of the operators.

$$\hat{H}_z = \chi \hat{J}_z^{(0)2}, \quad \hat{H}_{\text{prot}} = -\lambda \hat{J}^{(0)2}, \quad \hat{H}_{\text{env}}(t) = \frac{1}{\sqrt{N}} \sum_{k=0}^{N-1} g^k(t) \hat{J}_z^{(k)}, \quad (29)$$

where $g^k(t) = \frac{1}{\sqrt{N}} \sum_j h_j(t) e^{-i2\pi jk/N}$. With all of the possible states in the coupled basis and the operators defined for the full Hilbert space, we proceed to perturbation theory to solve for the time-evolution of the system.

4.2 Analytical solution - perturbation theory

To begin the calculation, we first define the complete set of Hamiltonians that describe the energy of the system

$$\hat{H}_{\text{tot}}(t) = \hat{H}_z + \hat{H}_{\text{prot}} + \hat{H}_{\text{env}}(t). \quad (30)$$

Then, we group the time-independent Hamiltonians into one term $\hat{H}_c \equiv \hat{H}_z + \hat{H}_{\text{prot}}$ and leave $\hat{H}_{\text{env}}(t)$ as the remaining time-dependent perturbation. Next, to make the strength of \hat{H}_{env} , we introduce a parameter Λ to indicate its amplitude. $\Lambda = \tilde{g}^k(t)/g^k(t)$ and assume $\Lambda \gg \lambda$. The unperturbed part \hat{H}_c is diagonalised by the coupled basis $|J, M, \beta\rangle$, and the eigenvalues are given by

$$\hat{H}_c |J, M, \beta\rangle = (\chi M^2 - \lambda J(J+1)) |J, M, \beta\rangle \equiv \xi_{J,M} |J, M, \beta\rangle. \quad (31)$$

We write the time evolved wavefunction as $|\psi(t)\rangle = \sum_{\alpha} a_{\alpha}(t) |\alpha\rangle$ where $\alpha = \{J, M, \beta\}$. By plugging $\psi(t)$ into the Schrodinger equation, the equation of the coefficient $a_{\alpha}(t)$ is obtained

$$a_{\alpha'}(t) - a_{\alpha'}(0) = \frac{\lambda}{i\hbar} \sum_{\alpha} \int_0^t a_{\alpha}(\tau) \tilde{\mathcal{H}}_{\text{env}}^{\alpha'\alpha}(\tau) e^{i\omega_{\alpha'\alpha}\tau/\hbar} d\tau, \quad (32)$$

where $\tilde{\mathcal{H}}_{\text{env}}^{\alpha'\alpha}(t) = \langle J', M', \beta' | \tilde{H}_{\text{env}}(t) | J, M, \beta \rangle$. We then expand the coefficients such that

$$a_{\alpha'}(t) = a_{\alpha'}^{(0)}(t) + \lambda a_{\alpha'}^{(1)}(t) + \lambda^2 a_{\alpha'}^{(2)}(t) + \dots \quad (33)$$

The approximations are listed below where the power of λ is represented by (#). We stop at the 2nd order because any higher order terms are not necessary for the scope of this project. This results in the following equations for the first two orders

$$(0): \quad a_{\alpha'}^{(0)}(t) - a_{\alpha'}^{(0)}(0) = 0 \quad (34)$$

$$(1): \quad a_{\alpha'}^{(1)}(t) = \frac{1}{i\hbar} \sum_{\alpha} \int_0^t a_{\alpha}^{(0)}(\tau) \tilde{\mathcal{H}}_{\text{env}}^{\alpha'\alpha}(\tau) e^{i\omega_{\alpha'\alpha}\tau/\hbar} d\tau \quad (35)$$

$$(2): \quad a_{\alpha'}^{(2)}(t) = \frac{1}{i\hbar} \sum_{\alpha} \int_0^t a_{\alpha}^{(1)}(\tau) \tilde{\mathcal{H}}_{\text{env}}^{\alpha'\alpha} e^{i\omega_{\alpha'\alpha}\tau/\hbar} d\tau. \quad (36)$$

Notice, since the initial state is unperturbed we set $a_{\alpha'}^{(l)}(0) = 0$ for $l > 0$. By plugging Eq.(35) into Eq.(36) we have

$$\begin{aligned} a_{\alpha'}(t) = & a_{\alpha'}^{(0)}(0) + \frac{1}{i\hbar} \sum_{\alpha \in \{\text{MPM}\}} \int_0^t a_{\alpha}^{(0)}(0) \mathcal{H}_{\text{env}}^{\alpha'\alpha}(\tau) e^{i\omega_{\alpha'\alpha}\tau/\hbar} d\tau \\ & + \frac{1}{i\hbar} \sum_{\alpha} \int_0^t \left(\frac{1}{i\hbar} \sum_{\alpha'' \in \{\text{MPM}\}} \int_0^{\tau} a_{\alpha''}^{(0)}(0) \mathcal{H}_{\text{env}}^{\alpha''\alpha'}(\tau') e^{i\omega_{\alpha''\alpha'}\tau'/\hbar} d\tau' \right) \mathcal{H}_{\text{env}}^{\alpha'\alpha}(\tau) e^{i\omega_{\alpha'\alpha}\tau/\hbar} d\tau. \end{aligned} \quad (37)$$

First, at time $t = 0$ the system lies in the ground state manifold. This means $a_{\alpha}^{(0)}(0) = 0$ for any $\alpha \notin \{\text{MPM}\}$. Second, we re-inserted the definition for $\tilde{\mathcal{H}}_{\text{env}}$. We are interested in the MPM subspace so we calculate the reduced density matrix using the projection operator

$\mathcal{P} = \sum_{\tilde{M}} |N/2, \tilde{M}\rangle\langle N/2, \tilde{M}|$. Thus,

$$\begin{aligned} \mathcal{P}\rho(t)\mathcal{P}^\dagger &= \sum_{M\tilde{M}} |N/2, M\rangle\langle N/2, M| \sum_{\alpha'} a_{\alpha'}(t) e^{-i\xi_{J'M'}t/\hbar} |J', M', \beta'\rangle \\ &\quad \sum_{\alpha''} a_{\alpha''}(t) e^{i\xi_{J''M''}t/\hbar} \langle J'', M'', \beta''|N/2, \tilde{M}\rangle |J'', M'', \beta''\rangle \langle N/2, \tilde{M}| \\ &= \sum_{M\tilde{M}} a_M(t) e^{-i\xi_{N/2, M}t/\hbar} |N/2, M\rangle\langle N/2, \tilde{M}| a_{\tilde{M}}(t) e^{i\xi_{N/2, \tilde{M}}t/\hbar}. \end{aligned} \quad (38)$$

The index $\alpha = \{J, M, \beta\}$ originally spanned the entire Hilbert space but is restricted to the ground state manifold, $\alpha = \{J = N/2, M\}$. To keep the space simple, let us write $\mathcal{P}|\psi(t)\rangle$ instead of $\mathcal{P}\rho(t)\mathcal{P}^\dagger$

$$\begin{aligned} \mathcal{P}|\psi(t)\rangle &= \sum_M \left[a_M^{(0)}(0) + \frac{1}{i\hbar} \int_0^t a_M^{(0)}(0) \langle N/2, M | \hat{H}_{\text{env}}(\tau) | N/2, M \rangle d\tau \right. \\ &\quad \left. - \frac{1}{\hbar^2} \sum_{J, \beta} \int_0^t \left(\int_0^\tau a_M^{(0)}(0) \langle J, M, \beta | \hat{H}_{\text{env}}(\tau') | N/2, M \rangle e^{i\omega_{JM\beta, M}\tau'/\hbar} d\tau' \right) \right. \\ &\quad \left. \langle N/2, M | \hat{H}_{\text{env}}(\tau) | J, M, \beta \rangle e^{i\omega_{M, JM\beta}\tau/\hbar} d\tau \right] e^{-i\xi_{N/2, \tilde{M}}t/\hbar} |N/2, M\rangle, \end{aligned} \quad (39)$$

where we use the fact that \hat{H}_{env} conserves M . We use integration by parts to simplify the last term in Eq.(39) and set $\hbar = 1$. The final result is given by

$$\begin{aligned} \mathcal{P}|\psi(t)\rangle &= \sum_M a_M^{(0)}(0) \left[1 - i \int_0^t \langle N/2, M | \hat{H}_{\text{env}}(\tau) | N/2, M \rangle d\tau \right. \\ &\quad \left. - \frac{1}{2} \sum_{J, \beta} \left| \int_0^t \langle N/2, M | \hat{H}_{\text{env}}(\tau) | J, M, \beta \rangle e^{i\omega_{J, \beta}\tau} d\tau \right|^2 \right] e^{-i\xi_{N/2, M}t} |N/2, M\rangle. \end{aligned}$$

We plug this back into the original density matrix equation as well as its complex conjugate. Each element of the density matrix $\rho_{M'\tilde{M}'}(t) = \langle N/2, M' | \rho(t) | N/2, \tilde{M}' \rangle$ is given by

$$\begin{aligned} \rho_{M\tilde{M}}(t) &= \rho_{M\tilde{M}}(0) e^{it\chi(M^2 - \tilde{M}^2)} \left(1 + i(\theta_M(t) - \theta_{\tilde{M}}(t)) - \frac{1}{2}(\gamma_M(t) + \gamma_{\tilde{M}}(t)) \right) \\ &\approx \rho_{M\tilde{M}}(0) e^{it\chi(M^2 - \tilde{M}^2)} e^{i(\theta_M(t) - \theta_{\tilde{M}}(t))} e^{-\frac{1}{2}(\gamma_M(t) + \gamma_{\tilde{M}}(t))}, \end{aligned} \quad (40)$$

where we denote the phase and decay rate as

$$\theta_M(t) = \int_0^t \langle N/2, M | \hat{H}_{\text{env}}(\tau) | N/2, M \rangle d\tau \quad (41)$$

$$\gamma_M(t) = \sum_{J, \beta} \left| \int_0^t \langle N/2, M | \hat{H}_{\text{env}}(\tau) | J, M, \beta \rangle e^{i\omega_{J, \beta}\tau} d\tau \right|^2. \quad (42)$$

5 Heisenberg XXZ model

In this section, we apply the many-body protected manifold to a lattice system. In particular, we consider the Heisenberg XXZ model. Ref.[[RJF⁺08](#)] has shown that this neighboring

interacting system can recover all-with-all interactions. We explain its analysis below. The Heisenberg XXZ model we consider reads

$$\hat{H}_{\text{lat}} = \hat{H}_H + \hat{H}_I = -\beta \sum_{i,\alpha} \hat{\sigma}_i^\alpha \hat{\sigma}_{i+1}^\alpha - \bar{\chi} \sum_i \hat{\sigma}_i^z \hat{\sigma}_{i+1}^z \quad (43)$$

where β and $\bar{\chi}$ represent neighboring interactions in x, y directions and z direction, respectively. The Heisenberg XXZ model can be mapped from Bose-Hubbard model by using a low-energy approximation Ref.[Hew97] and thus can be realized in a one-dimensional system of cold atoms. Similar to the previous section, the initial state is within the ground state manifold and we assume $\beta \gg \bar{\chi}$ which allows us to use perturbative analysis. Then as the system evolves, \hat{H}_H holds the dynamics within the ground-state manifold.

5.1 Collective spin operators

The first step is to write Eq.(43) in terms of collective spin operators. We first define their Fourier transform and inverse Fourier transform as

$$\hat{j}_z^{(k)} = \frac{1}{2} \sum_{n=0}^{N-1} \hat{\sigma}_n^z e^{\frac{2\pi i}{N} nk}, \quad (44)$$

$$\hat{\sigma}_n^z = \frac{2}{N} \sum_{k=0}^{N-1} \hat{j}_z^{(k)} e^{-\frac{2\pi i}{N} nk}. \quad (45)$$

Then we have the interaction Hamiltonian written in terms of the collective spin operators.

$$\begin{aligned} \hat{H}_I &= -\bar{\chi} \sum_{n=0}^{N-1} \left(\frac{2}{N} \sum_{k=0}^{N-1} \hat{j}_z^{(k)} e^{-\frac{2\pi i}{N} nk} \right) \left(\frac{2}{N} \sum_{k'=0}^{N-1} \hat{j}_z^{(-k')} e^{\frac{2\pi i}{N} (n+1)k'} \right) \\ &= -\frac{4\bar{\chi}}{N^2} \sum_{n=0}^{N-1} \sum_{k,k'=0}^{N-1} \hat{j}_z^{(k)} \hat{j}_z^{(-k')} e^{\frac{2\pi i}{N} n(k'-k)} e^{\frac{2\pi i}{N} k'} \\ &= -\frac{4\bar{\chi}}{N^2} \sum_{k=0}^{N-1} \hat{j}_z^{(k)} \hat{j}_z^{(-k)} e^{\frac{2\pi i}{N} k}, \end{aligned}$$

where $\sum_{n=0}^{N-1} \exp[2i\pi n(k' - k)/N] = 0$ for $k' \neq k$. Finally, the imaginary part is 0, and thus, we have

$$\hat{H}_I = -\frac{4\bar{\chi}}{N} \hat{j}_z^{(0)2} - \frac{4\bar{\chi}}{N} \sum_{k=1}^{N-1} \hat{j}_z^{(k)} \hat{j}_z^{(-k)} \cos\left(\frac{2\pi k}{N}\right). \quad (46)$$

We perform the same calculation for the total spin Hamiltonian

$$\hat{H}_H = -\frac{4\beta}{N} \sum_{\alpha} \hat{j}_{\alpha}^{(0)2} - \frac{4\beta}{N} \sum_{k=1}^{N-1} \sum_{\alpha} \hat{j}_{\alpha}^{(k)} \hat{j}_{\alpha}^{(-k)} \cos\left(\frac{2\pi k}{N}\right). \quad (47)$$

For $\beta \gg \bar{\chi}$, the term $-\frac{4\beta}{N} \sum_{\alpha} \hat{j}_{\alpha}^{(0)2}$ in \hat{H}_H forces the dynamics to be in the ground state manifold.

5.2 Projection into ground state manifold

We now project \hat{H}_I into the ground state manifold by using the projection operator

$$\mathcal{P} = \sum_M |N/2, M\rangle \langle N/2, M|. \quad (48)$$

Let us separate the Hamiltonian into its $k \neq 0$ and $k = 0$ subsets

$$\mathcal{P} [\hat{H}_I] = -\frac{4\bar{\chi}}{N} \mathcal{P} [\hat{J}_z^{(0)2}] - \frac{4\bar{\chi}}{N} \sum_{k=1}^{N-1} \mathcal{P} [\hat{J}_z^{(k)} \hat{J}_z^{(-k)}] \cos\left(\frac{2\pi k}{N}\right). \quad (49)$$

where $\mathcal{P} [\hat{O}] = \sum_{M\tilde{M}} |N/2, M\rangle\langle N/2, M| \hat{O} |N/2, \tilde{M}\rangle\langle N/2, \tilde{M}|$. Note, the first term in (49) does not change, so the second part is given by

$$\begin{aligned} \mathcal{P} [\hat{J}_z^{(k)} \hat{J}_z^{(-k)}] &= \sum_{M\tilde{M}} |N/2, M\rangle\langle N/2, M| \hat{J}_z^{(k)} \hat{J}_z^{(-k)} |N/2, \tilde{M}\rangle\langle N/2, \tilde{M}| \\ &= \sum_M |N/2, M\rangle\langle N/2, M| \hat{J}_z^{(k)} \hat{J}_z^{(-k)} |N/2, M\rangle\langle N/2, M|, \end{aligned} \quad (50)$$

where we use $[\hat{J}_z^{(0)}, \hat{J}_z^{(k)}] = 0$. Here, let us introduce a useful relation,

$$\sum_{k=0}^{N-1} \hat{J}_z^{(k)} \hat{J}_z^{(-k)} = \frac{1}{4} \sum_{k=0}^{N-1} \sum_{n=0}^{N-1} \sum_{m=0}^{N-1} \hat{\sigma}_n^z \hat{\sigma}_m^z e^{\frac{2\pi i}{N} k(n-m)} = \frac{N^2}{4}. \quad (51)$$

Next we project onto the identity above which returns

$$\sum_{k=1}^{N-1} \mathcal{P} [\hat{J}_z^{(k)} \hat{J}_z^{(-k)}] = \frac{N^2}{4} - \hat{J}_z^{(0)2}. \quad (52)$$

Below, we show $\mathcal{P} [\hat{J}_z^{(k)} \hat{J}_z^{(-k)}]$ is independent of k . We rewrite $\mathcal{P} [\hat{J}_z^{(k)} \hat{J}_z^{(-k)}]$ in the uncoupled basis,

$$\mathcal{P} [\hat{J}_z^{(k)} \hat{J}_z^{(-k)}] = \sum_{n,m=0}^{N-1} \langle N/2, M | \hat{\sigma}_m^z \hat{\sigma}_n^z | N/2, M \rangle e^{2i\pi k(n-m)/N}. \quad (53)$$

The above expectation value does not depend on position m, n due to the spin-symmetry of the state $|N/2, M\rangle$. For now, we can remove it from the sum and replace it with the constant C ,

$$\mathcal{P} [\hat{J}_z^{(k)} \hat{J}_z^{(-k)}] = C \sum_{n,m=0}^{N-1} e^{2i\pi k(n-m)/N}. \quad (54)$$

Next, we separate the sum into $n \neq m$ and $n = m$ subsets, because the latter is not dependent on k . The k -dependent part of the subset is

$$\sum_{n \neq m}^{N-1} e^{2i\pi k(n-m)/N}.$$

The indices of the summation span $-(N-1) \leq (n-m) \leq +(N-1)$ and provide a symmetry such that there are an equal amount of terms with $\exp[2i\pi k(n-m)/N]$ and $\exp[-2i\pi k(n-m)/N]$. So regardless of k , the terms will cancel. For example, for $N = 4$ we have $3e^{-\frac{i\pi k}{2}} + 3e^{\frac{i\pi k}{2}} + 2e^{-i\pi k} + 2e^{i\pi k} + e^{-\frac{3i\pi k}{2}} + e^{\frac{3i\pi k}{2}}$. This proves the projection Eq.(54) is not dependent on k . So, referring back to Eq.(52) we have

$$\mathcal{P} [\hat{J}_z^{(k)} \hat{J}_z^{(-k)}] = \frac{1}{N-1} \left(\frac{N^2}{4} - \hat{J}_z^{(0)2} \right). \quad (55)$$

The remainder of this calculation is straightforward as it is only a matter of plugging in what we have just derived. The result of the projection of \hat{H}_I into the MPM is

$$\mathcal{P} [\hat{H}_I] = \chi_e \hat{J}_z^{(0)2} + \frac{\bar{\chi}N}{N-1}, \quad (56)$$

where $\chi_e \equiv -\frac{4\bar{\chi}}{N-1}$. The first term shows that the Hamiltonian has the all-with-all interaction effectively. We now attempt to replicate this with the Heisenberg XXX model with a staggered field.

6 Results

In this section, we summarize our results. First, we justify why all-with-all interactions occur in a system with a nearest neighbour interacting Hamiltonian. Second, we apply techniques from Section 5 to the Heisenberg XXX model, in attempt to recover all-with-all interactions.

6.1 Recovering all-with-all interactions from Heisenberg XXZ

It is an important step to represent the neighboring interactions in the coupled basis. In this basis, we then separate the spin-symmetric part from the non-spin-symmetric part of \hat{H}_I . By confining the dynamics into the spin-symmetric space, the all-with-all interactions appear solely. We use this as a guideline for the Heisenberg XXX model in the following section.

6.2 Heisenberg XXX model with staggered field

We investigate the Heisenberg XXX model because in the presence of a staggered magnetic field it has been numerically shown to produce all-with-all interactions Ref.[[GUDB21](#)]. The difference between the XXX model and the XXZ model is simply the uniformity in the strength of interactions across all components $\{x, y, z\}$. Thus, the Heisenberg XXX model we consider reads

$$\hat{H} = \frac{\beta}{4} \sum_{i=1}^{N-1} \left(\hat{\sigma}_i^x \hat{\sigma}_{i+1}^x + \hat{\sigma}_i^y \hat{\sigma}_{i+1}^y + \hat{\sigma}_i^z \hat{\sigma}_{i+1}^z \right) + \frac{\alpha}{2} \sum_{i=0}^{N-1} (-1)^i \hat{\sigma}_i^z, \quad (57)$$

where we represent the first term with \hat{H}_H and the second term with \hat{H}_{SF} . Following Section 5, we first convert the Pauli operators in Eq.(57) to their respective collective spin operators. Notice, \hat{H}_H in both the XXZ and XXX models are defined identically and so we can simply use Eq.(47). Similarly, we use Fourier transform of \hat{H}_{SF} , which results in the total Hamiltonian

$$\hat{H} = \frac{\beta}{N} \sum_{\alpha} \sum_{k=0}^{N-1} \hat{J}_{\alpha}^{(k)} \hat{J}_{\alpha}^{(-k)} \cos\left(\frac{2\pi k}{N}\right) + \frac{\alpha}{N} \sum_{j=0}^{N-1} \sum_{k=0}^{N-1} (-1)^j \hat{J}_z^{(k)} e^{-\frac{2\pi i}{N}jk}. \quad (58)$$

We make the assumption that $\beta \gg \alpha$, which causes \hat{H}_H to force the system in the ground-state manifold. This is the same approximation as Ref.[[GUDB21](#)]. We calculate $\mathcal{P}[\hat{H}_{SF}]$, and let us look at \hat{H}_{SF} shown in Eq.(58). Without the the stagger term $(-1)^j$, the summation of the position j gives 0 except for the case of $j = 0$, and thus only $\hat{J}_z^{(0)}$ remains. On the other hand, with the stagger term, only the term of $j = N/2$ remains, and $\hat{J}_z^{(N/2)}$ survives. Figure 3 displays $\sum_{j=0}^{N-1} (-1)^j \exp[-2i\pi jk/N]$ for $N = 4$, where the

blue/orange dots represent the cases without/with the $(-1)^j$ term, respectively. As a result, the stagger field is given by

$$\hat{H}_{SF} = \alpha \hat{J}_z^{(N/2)}. \quad (59)$$

The issue here is that the above is a collective spin operator where $k \neq 0$. These operators only connect states outside of the MPM, so when projecting Eq.(59) into the MPM we have 0.

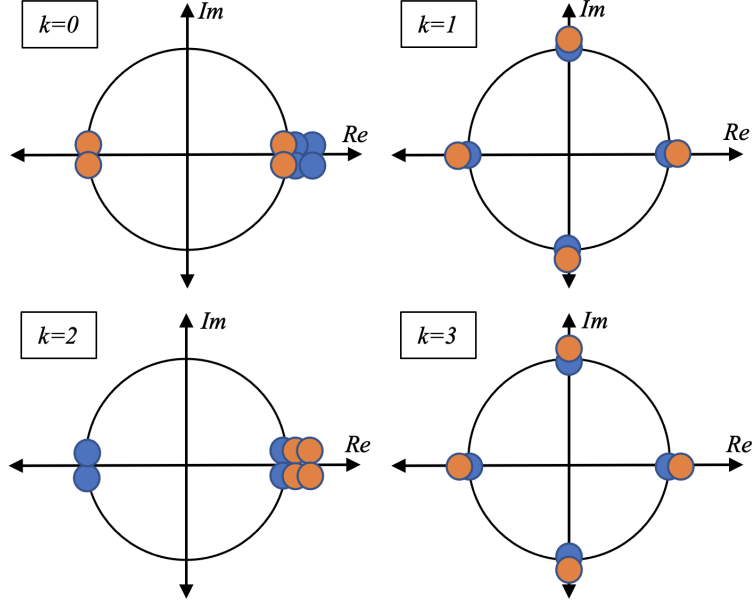


Figure 3: Unit circle analysis with $N = 4$, where the blue dots represent the case with the stagger term and the orange dots represent the case without the stagger term.

7 Conclusion

In conclusion, the primary objective of this thesis is to recover all-with-all interactions from the Heisenberg XXX model. We thoroughly review the generation of maximally entangled spin states first with the infinite range one-axis twisting Hamiltonian. We then derive the coherent spin states and apply the OAT Hamiltonian. Then, to show the dynamics, we plot the Husimi quasi-probability distribution.

Next, we closely follow the methods in the article *Many-body protected entanglement generation in interacting spin systems* Ref.[RJF⁺08]. This entails the addition of single-particle dephasing which models the decoherence of the quantum system. From which, we apply the many-body protected manifold to show how the entanglement generation can be protected from decoherence. Then, applying this technique to the XXZ model, we recover the all-with-all interactions which are generated from the spin-symmetric properties of the coupled basis.

Finally, we apply these methods to the Heisenberg XXX model with a staggered field which was numerically demonstrated to produce all-with-all interactions in Ref.[GADB21]. However, we find that applying the same approach straightforwardly only recovers $\hat{H}_{SF} = \alpha \hat{J}_z^{(N/2)}$, which does not entail all-with-all interactions when projected into the spin symmetric space. One thing we can check is whether the spherically symmetric Hamiltonian

\hat{H}_H is affected by $\hat{H}_{SF} = \alpha \hat{J}_z^{(N/2)}$. The \hat{H}_H has a non-spin-symmetric part, and the stagger fields may affect this part.

Future research

There are two potential methods for recovering all-with-all interactions from the Heisenberg XXX model with a staggered field. The first thing is to can further investigate the role of the total spin Hamiltonian as addressed above. The second thing is to study they entanglement generation from the perspective of spontaneous symmetry breaking. It has been reported that spontaneous symmetry breaking cause one-axis twisting in the Heisenberg XXZ model with a staggered field in Ref.[[CMRdSVR22](#)] and perhaps this can applied to the XXX model with a staggered field.

Bibliography

- [AAA⁺13] Junaid Aasi, Joan Abadie, BP Abbott, Richard Abbott, TD Abbott, MR Abernathy, Carl Adams, Thomas Adams, Paolo Addesso, RX Adhikari, et al. Enhanced sensitivity of the ligo gravitational wave detector by using squeezed states of light. *Nature Photonics*, 7(8):613–619, 2013.
- [ACGT72] F. T. Arecchi, Eric Courtens, Robert Gilmore, and Harry Thomas. Atomic coherent states in quantum optics. *Phys. Rev. A*, 6:2211–2237, Dec 1972.
- [BZ06] Immanuel Bloch and Peter Zoller. Focus on cold atoms in optical lattices. *New Journal of Physics*, 8(8):E02, 2006.
- [CMRdSVR22] Tommaso Comparin, Fabio Mezzacapo, Martin Robert-de Saint-Vincent, and Tommaso Roscilde. Scalable spin squeezing from spontaneous breaking of a continuous symmetry. *arXiv preprint arXiv:2202.08607*, 2022.
- [Dic54] Robert H Dicke. Coherence in spontaneous radiation processes. *Physical review*, 93(1):99, 1954.
- [GUDB21] Karol Gietka, Ayaka Usui, Jianqiao Deng, and Thomas Busch. Simulating the same physics with two distinct hamiltonians. *Physical Review Letters*, 126(16):160402, 2021.
- [Hew97] Alexander Cyril Hewson. *The Kondo problem to heavy fermions*. Number 2. Cambridge university press, 1997.
- [HGH⁺12] Klaus Hornberger, Stefan Gerlich, Philipp Haslinger, Stefan Nimmrichter, and Markus Arndt. Colloquium: Quantum interference of clusters and molecules. *Reviews of Modern Physics*, 84(1):157, 2012.
- [HMP⁺97] Susanna F Huelga, Chiara Macchiavello, Thomas Pellizzari, Artur K Ekert, Martin B Plenio, and J Ignacio Cirac. Improvement of frequency standards with quantum entanglement. *Physical Review Letters*, 79(20):3865, 1997.
- [KU93] Masahiro Kitagawa and Masahito Ueda. Squeezed spin states. *Phys. Rev. A*, 47:5138–5143, Jun 1993.
- [LBY⁺15] Andrew D Ludlow, Martin M Boyd, Jun Ye, Ekkehard Peik, and Piet O Schmidt. Optical atomic clocks. *Reviews of Modern Physics*, 87(2):637, 2015.
- [LLMP19] Benjamin J Lawrie, Paul D Lett, Alberto M Marino, and Raphael C Pooser. Quantum sensing with squeezed light. *Acs Photonics*, 6(6):1307–1318, 2019.
- [LP18] Benjamin J Lawrie and Raphael C Pooser. Atomic force microscopy beyond the standard quantum limit. In *2018 Conference on Lasers and Electro-Optics (CLEO)*, pages 1–2. IEEE, 2018.
- [MBPL08] Alberto M. Marino, Vincent Boyer, Raphael C. Pooser, and Paul D. Lett. Production of entangled images by four-wave mixing. *Opt. Photon. News*, 19(12):45–45, Dec 2008.
- [MWSN11] Jian Ma, Xiaoguang Wang, Chang-Pu Sun, and Franco Nori. Quantum spin squeezing. *Physics Reports*, 509(2-3):89–165, 2011.
- [PPCS⁺20] Edwin Pedrozo-Peñafiel, Simone Colombo, Chi Shu, Albert F Adiyatullin, Zeyang Li, Enrique Mendez, Boris Braverman, Akio Kawasaki, Daisuke Akamatsu, Yanhong Xiao, et al. Entanglement on an optical atomic-clock transition. *Nature*, 588(7838):414–418, 2020.
- [RBH01] Jean-Michel Raimond, M Brune, and Serge Haroche. Manipulating quantum entanglement with atoms and photons in a cavity. *Reviews of Modern Physics*, 73(3):565, 2001.

- [Rey21] Ana Maria Rey. Ultra-cold bosonic atoms in optical lattices: An overview. *Revista de la Academia Colombiana de Ciencias Exactas, Físicas y Naturales*, 45(176):666–696, 2021.
- [RGK⁺14] AM Rey, AV Gorshkov, CV Kraus, MJ Martin, M Bishof, MD Swallows, X Zhang, C Benko, J Ye, ND Lemke, et al. Probing many-body interactions in an optical lattice clock. *Annals of Physics*, 340(1):311–351, 2014.
- [Rip16] Juan José García Ripoll. Studying spin squeezing in mathematica, 2016.
- [RJF⁺08] AM Rey, L Jiang, M Fleischhauer, E Demler, and MD Lukin. Many-body protected entanglement generation in interacting spin systems. *Physical Review A*, 77(5):052305, 2008.
- [SHH21] Stuart S Szigeti, Onur Hosten, and Simon A Haine. Improving cold-atom sensors with quantum entanglement: Prospects and challenges. *Applied Physics Letters*, 118(14):140501, 2021.
- [TKL⁺00] Quentin A Turchette, BE King, D Leibfried, DM Meekhof, CJ Myatt, MA Rowe, CA Sackett, CS Wood, WM Itano, C Monroe, et al. Heating of trapped ions from the quantum ground state. *Physical Review A*, 61(6):063418, 2000.
- [WPW99] Carl E Wieman, David E Pritchard, and David J Wineland. Atom cooling, trapping, and quantum manipulation. *Reviews of Modern Physics*, 71(2):S253, 1999.
- [XWK87] Min Xiao, Ling-An Wu, and H Jeffrey Kimble. Precision measurement beyond the shot-noise limit. *Physical review letters*, 59(3):278, 1987.
- [Zur02] Wojciech H Zurek. Decoherence and the transition from quantum to classical-revisited. *Los Alamos Science*, 27:86–109, 2002.

A Coherent spin states

Let's first rotate the frame of reference about the z -axis,

$$J_z = J_z, \quad (60)$$

$$J_n = J_x \sin \phi - J_y \cos \phi, \quad (61)$$

$$J_k = J_x \cos \phi + J_y \sin \phi. \quad (62)$$

Now we want to rotate about the new arbitrary n -axis by the angle θ

$$\begin{aligned} R_{\theta, \phi} &= e^{-i\theta J_n} \\ &= e^{-i\theta(J_x \sin \phi - J_y \cos \phi)} \\ &= e^{\xi J_+ - \xi^* J_-}, \end{aligned} \quad (63)$$

where $\xi = \frac{\theta}{2} e^{-i\phi}$, and $J_x = \frac{1}{2}(J_+ + J_-)$, and $J_y = \frac{1}{2i}(J_+ - J_-)$. Now that we have the rotation operator, we apply it to the ground (or excited) state, which gives us the coherent spin state. Again, it is helpful to notice the direct similarities between the coherent spin state and coherent field state

$$|\theta, \phi\rangle = R_{\theta, \phi} |J, -J\rangle \leftrightarrow |\alpha\rangle = \exp[\alpha a^\dagger - \alpha^* a] |0\rangle.$$

Our goal is to rotate the operators $J_{-,+}$ which are dependent on $J_{n,k}$. So let us begin with rotating the latter. We can take the definitions from the ϕ -rotation, and apply them to the θ -rotation. Let $R_{\theta, \phi} J_\alpha R_{\theta, \phi}^{-1} = J'_\alpha$

$$J'_n = J_n, \quad (64)$$

$$J'_k = J_k \cos \theta + J_z \sin \theta, \quad (65)$$

$$J'_z = J_k \sin \theta - J_z \cos \theta. \quad (66)$$

Next, we find the ladder operators defined by the spin operators and the definitions of J_x and J_y given above, but first

$$J_k = \frac{1}{2} (J_+ e^{-i\phi} + J_- e^{i\phi}) \quad (67)$$

$$J_n = \frac{i}{2} (J_- e^{-i\phi} - J_+ e^{i\phi}). \quad (68)$$

Now we find J_+ and J_-

$$J_+ = e^{i\phi} (J_k - iJ_n) \quad (69)$$

$$J_- = e^{-i\phi} (J_k + iJ_n). \quad (70)$$

Finally, the rotated ladder operators are given by

$$\begin{aligned} J'_+ &= e^{i\phi} (J'_k - iJ'_n) = e^{i\phi} [(J_k \cos \theta + J_z \sin \theta) - i(J_n)] \\ &= e^{i\phi} [J_+ e^{-i\phi} \cos^2(\theta/2) - J_- e^{i\phi} \sin^2(\theta/2) + J_z \sin(\theta)], \\ J'_- &= e^{-i\phi} [J_- e^{i\phi} \cos^2(\theta/2) - J_+ e^{-i\phi} \sin^2(\theta/2) + J_z \sin(\theta)]. \end{aligned}$$

Now we can properly define the coherent spin state, which is the rotated ground Dicke state where $J_- |J, -J\rangle = 0$. We start with projecting the rotation operator to the left of this equation

$$R_{\theta, \phi} (J_- |J, -J\rangle) = 0.$$

We also know

$$J_- (R_{\theta,\phi}^{-1} R_{\theta,\phi}) |J, -J\rangle = J_- \otimes \mathbb{1} |J, -J\rangle = J_- |J, -J\rangle.$$

Therefore,

$$(R_{\theta,\phi} J_- R_{\theta,\phi}^{-1}) R_{\theta,\phi} |J, -J\rangle = 0,$$

and from the definition of a CSS: $|\theta, \phi\rangle = R_{\theta,\phi} |J, -J\rangle$ we have the following eigenvalue equation for the coherent spin state

$$J'_- |\theta, \phi\rangle = e^{-i\phi} [J_- e^{i\phi} \cos^2(\theta/2) - J_+ e^{-i\phi} \sin^2(\theta/2) + J_z \sin(\theta)] |\theta, \phi\rangle = 0. \quad (71)$$

Furthermore, we know the total angular momentum of the system eigenvalue equation $J^2 |J, M\rangle = J(J+1) |J, M\rangle$. Since the CSS is just a rotation of the initial ground state, the eigenfunction for the total spin will still apply

$$J^2 |\theta, \phi\rangle = J(J+1) |\theta, \phi\rangle. \quad (72)$$

We would now like expand the coherent spin state in terms of the Dicke states, similar to the definition for a coherent field state $|\alpha\rangle = \sum \frac{1}{\sqrt{N}} e^{-|\alpha|^2/2} \alpha^n |n\rangle$. We begin with the definition of the rotation operator acting on the ground state

$$|\theta, \phi\rangle = R_{\theta,\phi} |J, -J\rangle.$$

We can redefine the rotation operator using the disentangling theorem

$$e^{\tau J_+} e^{\ln(1+|\tau|^2) J_z} e^{-\tau^* J_-} |J, -J\rangle, \quad (73)$$

where $\tau = \tan(\frac{\theta}{2}) e^{i\phi}$. Next, breaking this into three sections, we begin with the right-most term

$$e^{-\tau^* J_-} |J, -J\rangle = \sum_{n=0}^{\infty} \frac{(-\tau^* J_-)^n}{n!} |J, -J\rangle = |J, -J\rangle,$$

because the first term of the series is 1, and the rest are annihilated by the J_- operator. Now, the middle term applied to the state is

$$e^{\ln(1+|\tau|^2) J_z} |J, -J\rangle = (1 + |\tau|^2)^{J_z} |J, -J\rangle = (1 + |\tau|^2)^{-J} |J, -J\rangle.$$

Now, we find the left-most term

$$e^{\tau J_+} |J, -J\rangle = \sum_{n=0}^{\infty} \frac{(\tau J_+)^n}{n!} |J, -J\rangle.$$

Note, we set better bounds for n because of our familiarity with the system. For instance, we know when $n = J + M$ the upper bound should be $M = J$ because this would give us $(J_+)^{2J} |J, -J\rangle = |J, J\rangle$. And the lower bound is $M = -J$ because $(J_+)^0 |J, -J\rangle = |J, -J\rangle$

$$\sum_{M=-J}^J \frac{\tau^{J+M}}{(J+M)!} J_+^{J+M} |J, -J\rangle.$$

So now put together all three terms we just solved for separately

$$|\theta, \phi\rangle = \sum_{M=-J}^J \frac{1}{(1 + |\tau|^2)} \frac{\tau^{J+M}}{(J+M)!} J_+^{J+M} |J, -J\rangle.$$

Now we substitute the definition for Dicke states into this equation. This gives us the final definition of a coherent spin state

$$|\theta, \phi\rangle = \sum_{M=-J}^J \frac{1}{(1 + |\tau|^2)} \binom{2J}{M+J}^{1/2} \tau^{J+M} |J, M\rangle. \quad (74)$$

B Expectation value of collective spin operator

The definition for the time evolution of the ladder operator is $\hat{J}_+(t) = \hat{U}^\dagger \hat{J}_+(0) \hat{U}$. We want to flip U^\dagger and $J_+(0)$ in order to get $U^\dagger U = \mathbb{1}$

$$\sum_{k=0}^{\infty} \frac{(i\chi t)^k}{k!} (J_z)^{2k} (J_+).$$

Now we need the commutation relations between J_z and J_+ to simplify. By definition

$$\begin{aligned} [J_z, J_+] &= J_+, \\ J_z J_+ - J_+ J_z &= J_+, \\ J_z J_+ &= J_+ + J_+ J_z = J_+ (J_z + 1). \end{aligned}$$

Let's apply the J_z operator again

$$(J_z)^2 J_+ = J_z J_+ (J_z + 1) = J_+ (J_z + 1)^2.$$

Thus, we notice the pattern

$$(J_z)^{2k} J_+ = J_+ (J_z + 1)^{2k}.$$

Therefore, plugging back into the exponential function

$$\sum_{k=0}^{\infty} \frac{(i\chi t)^k}{k!} (J_z)^{2k} (J_+) = (J_+) \sum_{k=0}^{\infty} \frac{(i\chi)^k}{k!} (J_z + 1)^{2k} = (J_+) e^{i\chi t (J_z + 1)^2}.$$

Now we can multiply this by the R.H.S.

$$J_+(t) = U^\dagger J_+(0) U = J_+(0) e^{i2\chi t (J_z + 1/2)}. \quad (75)$$

Now we find the expectation value

$$\begin{aligned} &= \langle J, M' | 2^{-J} \sum_{M'=-J}^J \binom{2J}{J+M'}^{1/2} [J_+(0) e^{i2\chi t (J_z + 1/2)}] 2^{-J} \sum_{M=-J}^J \binom{2J}{J+M}^{1/2} |J, M\rangle \\ &= \langle J, M' | 2^{-J} \sum_{M'=-J}^J \binom{2J}{J+M'}^{1/2} [\sqrt{J(J+1) - M(M+1)} e^{i2\chi t (M+1/2)}] 2^{-J} \\ &\quad \times \sum_{M=-J}^J \binom{2J}{J+M}^{1/2} |J, M+1\rangle \\ &= 2^{-2J} \sum_{M=-J}^J \binom{2J}{J+M}^{1/2} \binom{2J}{J+M+1}^{1/2} \sqrt{J(J+1) - M(M+1)} e^{i2\chi t (M+1/2)} \\ &= 2^{-2J} \sum_{M=-J}^J \frac{(2J)!}{(J-M)!(J+M)!} (J-M) e^{i\mu(M+1/2)}. \end{aligned}$$

Currently, in this form we have the same numerical results as Kitagawa. However, to simplify the expression further, we need to make some adjustments to the summation. The first thing we can do is shift the summation: let $M' = J - M$

$$= 2^{-2J} \sum_{M'=1}^{2J} \frac{(2J)!}{(2J-M')!(M')!} (M') e^{i\mu(J-M'+1/2)}.$$

Note, we neglected the first term of the sum since it will be equal to 0. We notice a factorial term divided by itself

$$= 2^{-2J} \sum_{M'=1}^{2J} \frac{(2J)!}{(2J-M')!(M'-1)!} e^{i\mu(J-M'+1/2)}.$$

Next, we notice the terms from $M' = 1$ to $M' = J$ are equal to the complex conjugates of the terms from $M' = J + 1$ to $M' = 2J$. Because we only consider the real terms, we can make the upper bound of the sum $M' = J$ and multiply the sum by 2. Furthermore, we can reduce the exponential to its real term

$$= 2 \cdot 2^{-2J} \sum_{M'=1}^J \frac{(2J)!}{(2J-M')!(M'-1)!} \cos(\mu(J-M'+1/2)).$$

Next, to set the lower bound equal to zero again, we can create another variable $M'' = M' - 1$. This will give the new expression

$$= 2 \cdot 2^{-2J} \sum_{M''=0}^J \frac{(2J)!}{(2J-M''-1)!(M'')!} \cos(\mu(J-M''-1/2)).$$

We have the following definition for a combination

$$\binom{2J-1}{M''} = \frac{(2J-1)!}{(2J-1-M'')!(M'')!} = \frac{(2J-1)!}{(2J-1-M'')!(M'')!}. \quad (76)$$

Therefore,

$$\frac{(2J)!}{(2J-M''-1)!(M'')!} = \frac{(2J-1)!}{(2J-M''-1)!(M'')!} (2J).$$

So now our equation is

$$\langle J_+ \rangle = \frac{J}{2^{2(J-1)}} \sum_{M''=0}^J \binom{2J-1}{M''} \cos\left(\frac{\mu}{2}(2J-2M''-1)\right).$$

This can be simplified even further using a trigonometric power formula

$$\cos^{2n-1} x = \frac{1}{2^{2(n-1)}} \sum_{k=0}^n \binom{2n-1}{k} \cos[(2n+1-2k)x]. \quad (77)$$

And because $\langle J_x \rangle = \text{Re}[\langle J_+ \rangle]$ we have the final definition for the expectation value of the x -spin operator in a squeezed coherent spin state

$$\langle J_x \rangle = J \cos^{2J-1} \frac{\mu}{2}. \quad (78)$$

C Fidelity calculation

First we provide the proof for the Gaussian variable simplification in (24). The overline will be restricted to the density matrix $\rho(t_0)$ because only it contains the Gaussian variables

$$\overline{\hat{\rho}(t_0)} = \sum_{k,l} \rho_{k,l}(0) e^{-i\chi t_0/4} [(\sum_i s_i^k)^2 - (\sum_i s_i^l)^2] e^{-i/2 \sum_i \int_0^{t_0} d\tau h_i(\tau)(s_i^k - s_i^l)} \left| n^{(k)} \right\rangle \left\langle n^{(l)} \right|. \quad (79)$$

The following simplification $\overline{e^{-i/2 \sum_i \int_0^{t_0} d\tau h_i(\tau)(s_i^k - s_i^l)}} = e^{-\frac{1}{2}\Gamma(t_0) \sum_i (s_i^k - s_i^l)}$ is made with the following justification. Consider an N -particle system

$$\begin{aligned}
&= \overline{e^{-i/2 \sum_i \int_0^{t_0} d\tau h_i(\tau)(s_i^k - s_i^l)}} \\
&= \overline{e^{-i/2 [\int_0^{t_0} d\tau h_1(\tau)(s_1^k - s_1^l) + \int_0^{t_0} d\tau h_2(\tau)(s_2^k - s_2^l) + \dots]} \\
&= \overline{e^{-i/2 \int_0^{t_0} d\tau h_1(\tau)(s_1^k - s_1^l)} e^{-i/2 \int_0^{t_0} d\tau h_2(\tau)(s_2^k - s_2^l)} \dots} \\
&= e^{-\frac{1}{2}\Gamma(t_0)(s_1^k - s_1^l)} e^{-\frac{1}{2}\Gamma(t_0)(s_2^k - s_2^l)} \dots \\
&= e^{-\frac{1}{2}\Gamma(t_0) \sum_i (s_i^k - s_i^l)}.
\end{aligned}$$

Therefore, the density matrix equation with decoherence is now

$$\begin{aligned}
\overline{\hat{\rho}(t_0)} &= \sum_{k,l} \rho_{k,l}(0) e^{-i\chi t_0/4 [(\sum_i s_i^k)^2 - (\sum_i s_i^l)^2]} e^{-\frac{1}{2}\Gamma(t) \sum_i (s_i^k - s_i^l)} |n^{(k)}\rangle \langle n^{(l)}| \\
&= \sum_{k,l} \rho_{k,l}(t_0) |n^{(k)}\rangle \langle n^{(l)}|.
\end{aligned}$$

Now we provide the proof for (25) – the GHZ state in the uncoupled basis. To do this, we consider the state where there is no decoherence and the time is also $t = t_0$. So let us begin with the time evolution of the initial state $|\psi\rangle = \sum_i c_i |\psi_i\rangle$,

$$\begin{aligned}
|\psi(t)\rangle &= U(t) |\psi\rangle = \sum_k c_k(0) e^{-i\chi t/4 (\sum_i \sigma_i^z)^2} |n^{(k)}\rangle \\
&= \sum_k c_k(0) e^{-i\chi t/4 (\sum_i s_i^k)^2} |n^{(k)}\rangle.
\end{aligned}$$

Next, we let $t = t_0$ because this is the time when the state is maximally entangled

$$\begin{aligned}
|\psi_x^{\text{GHZ}}\rangle &= \sum_k c_k(0) e^{-i\chi t_0/4 (\sum_i s_i^k)^2} |n^{(k)}\rangle \\
&= \sum_k c_k(t_0) |n^{(k)}\rangle.
\end{aligned} \tag{80}$$

Now we provide the proof for the fidelity equation (26)

$$\begin{aligned}
\mathcal{F}(t_0) &= \sum_j \langle n^{(j)} | c_j^*(t_0) \sum_{k,l} \rho_{k,l}(t_0) |n^{(k)}\rangle \langle n^{(l)}| \sum_m c_m(t_0) |n^{(m)}\rangle \\
&= \sum_j \langle n^{(j)} | c_j^*(t_0) \sum_{k,l} \rho_{k,l}(t_0) c_l(t_0) |n^{(k)}\rangle \\
&= \sum_{k,l} c_k^*(t_0) \rho_{k,l}(t_0) c_l(t_0).
\end{aligned}$$

Now we plug back in the coefficients and let $c_k^*(0)c_l(0) = \rho_{k,l}(0)$

$$\begin{aligned}
\mathcal{F}(t_0) &= \sum_{k,l} \rho_{k,l}(0) e^{i\chi t_0/4 (\sum_i s_i^k)^2} e^{-i\chi t_0/4 (\sum_i s_i^l)^2} \rho_{k,l}(0) \\
&\quad \times e^{-i\chi t_0/4 [(\sum_i s_i^k)^2 - (\sum_i s_i^l)^2]} e^{-\frac{1}{2}\Gamma(t_0) \sum_i (s_i^k - s_i^l)} \\
&= \sum_{k,l} \rho_{k,l}^2(0) e^{-\frac{1}{2}\Gamma(t_0) \sum_i (s_i^k - s_i^l)}.
\end{aligned}$$

At $t = 0$, the atoms are all polarized in the x direction, so $\rho_{k,l}(0) = 2^{-N}$. Furthermore, we include an absolute value around the eigenvalues as to maintain the fact that $\Gamma(t_0)$ is always negative

$$\mathcal{F}(t_0) = 2^{-2N} \sum_{k,l}^{2N} e^{-\frac{1}{2}\Gamma(t_0) \sum_i |s_i^k - s_i^l|}. \quad (81)$$

To simplify this, we decompose it into the possible outcomes for each index k, l . First, we know are a number of terms where

$$\sum_i |s_i^k - s_i^l| = 0.$$

The only time when this is possible is when $k = l$, because the two states are identical. The next possibility is

$$\sum_i |s_i^k - s_i^l| = 2.$$

This happens when all the spins are aligned in the same direction between the two states except exactly one. Continuing this pattern, we see the maximum amount is

$$\sum_i |s_i^k - s_i^l| = 2N.$$

We arrive to this value because every spin of one state is oppositely aligned with the spin of the other state. The next step is to calculate the number of times each of these scenarios occur when applying the sum $\sum_{k,l}^{2N}$. The first term is simple, because we know the amount of times $k = l$ when expanding the sum is 2^N times. So, building the fidelity equation

$$\begin{aligned} \mathcal{F}(t_0) &= 2^{-2N} \left(2^N e^{-\frac{1}{2}\Gamma(t_0)*0} + \dots \right) \\ &= 2^{-2N} \left(2^N + \dots \right). \end{aligned}$$

The next term when the spins are all in the same direction except exactly one happens $N2^N$ times. This can be explained by the fact that for every state, the i th particle can be flipped once to achieve 2. So we multiply the number of states 2^N by N

$$\mathcal{F}(t_0) = 2^{-2N} \left(2^N + 2^N N e^{-\Gamma(t_0)} + \dots \right).$$

Moving forward, we can see this process of determining the amount of spins flipped per state can be modeled with the combination formula. For instance, if we have a state of $N = 4$, and we want to determine how many possibilities there are for an arbitrary state to have exactly 2 spins flipped, we use ${}_4C_2$. Thus, the fidelity becomes

$$\begin{aligned} \mathcal{F}(t_0) &= 2^{-2N} \left(2^N + 2^N ({}_N C_1) e^{-\Gamma(t_0)} + \dots + 2^N ({}_N C_N) e^{-N\Gamma(t_0)} \right) \\ &= 2^{-N} \left(1 + ({}_N C_1) e^{-\Gamma(t_0)} + \dots + ({}_N C_N) e^{-N\Gamma(t_0)} \right) \\ &= 2^{-N} \left(\sum_{n=0}^N {}_N C_n e^{-n\Gamma(t_0)} \right) \\ &= 2^{-N} \left(1 + e^{-\Gamma(t_0)} \right)^N \\ &= \left(\frac{1 + e^{-\Gamma(t_0)}}{2} \right)^N. \end{aligned}$$